# Multiscale kinetic model for polarization switching in ferroelectric polymer thin films

Rajeev Ahluwalia,[1,2] Michael B. Sullivan,[3] David J. Srolovitz,[1,2,4] Jian Wei Zheng,[3] and Alfred C. H. Huan[2,5]
[1]*Materials Theory and Simulation Laboratory, Institute of High Performance Computing, A*STAR (Agency for Science, Technology and Research), Singapore 117528, Singapore*
[2]*Institute of Materials Research and Engineering, A*STAR (Agency for Science, Technology and Research), Singapore 117602, Singapore*
[3]*Computational Materials Science and Engineering Programme, Institute of High Performance Computing, A*STAR (Agency for Science, Technology and Research), Singapore 117528, Singapore*
[4]*Department of Physics, Yeshiva University, New York, New York 10033, USA*
[5]*Division of Physics and Applied Physics, School of Physical and Mathematical Sciences, Nanyang Technological University, Singapore 637616, Singapore*
(Received 10 March 2008; revised manuscript received 5 June 2008; published 12 August 2008)

Polarization switching in ferroelectric polymers is studied using a multiscale framework. A continuum Landau-Ginzburg-Devonshire model for a first-order phase transition is parametrized for ideal all trans chains of P(VDF-TrFE) (70:30) copolymers using data obtained from molecular-dynamics (MD) simulations. Thermal fluctuations and kinetics are accounted for by using a time-dependent Ginzburg-Landau model where the length and time scales, as well as the thermal noise amplitude, are also set from MD simulations. This method is used to investigate the nature of polarization switching in ferroelectric polymers and to test recent claims that ultrathin ferroelectric polymer films undergo intrinsic switching. Our simulations show that for a defect-free system, domain nucleation due to thermal fluctuations prevents homogeneous switching of the polarization, even at very small thicknesses. However, this nucleation does not substantially decrease the coercive field compared to the intrinsic value.

DOI: 10.1103/PhysRevB.78.054110 PACS number(s): 77.80.Dj

## I. INTRODUCTION

It is well known that polyvinylidene fluoride (PVDF) and its copolymers with trifluoroethylene (TrFE) exhibit paraelectric to ferroelectric transitions.[1,2] These polymers are attracting increasing attention due to potential applications in piezoelectric,[3] as well as memory, devices.[4] Many of these applications rest on the ability of the polarization to switch upon application of an external electric field. Polarization switching has been particularly widely studied, theoretically, for ferroelectric perovskite thin films.[5,6] However, little attention has been devoted to understand the mechanism of polarization switching in organic thin films, such as those of P(VDF-TrFE) copolymers, where the interatomic interactions are fundamentally different from those in perovskites.

Polarization switching in ferroelectrics is a complex process that is governed by macroscopic thermodynamics as well as the microscopic kinetics of the polymer chains. At the atomistic scale, molecular-dynamics (MD) simulations have been used to study PVDF and related copolymers. The MSXX force field was originally parametrized specifically for PVDF by Karasawa and Goddard[7] and was later modified by Abe *et al.*[8] The latter force field has been used extensively to study the polarization of PVDF with TrFE.[9] In addition, there has been a number of other studies using related force fields to explore the behavior of PVDF.[10] However, for calculating the macroscopic properties, such as the polarization-electric field (P-E) loops, a purely atomistic approach is clearly inadequate since these would require very large simulation cells. On the other hand, there are phenomenological continuum models such as the Landau-Ginzburg-Devonshire (LGD) theory and the time-dependent Ginzburg-Landau (TDGL) model, which can describe the P-E response incorporating both thermodynamics and kinetics. However, these models have several phenomenological parameters that must be determined for a given material to make quantitative predictions. A complete analysis of this problem therefore warrants a multiscale framework that combines information from the molecular level with a mesoscale kinetic model for modeling domain dynamics. In this paper, we propose a multiscale kinetic framework to predict the P-E loops for ferroelectric polymers, taking into account thermodynamics as well as the role of thermal fluctuations.

An important advancement in the field of ferroelectric polymers has been the development of highly crystalline ordered nanoscale Langmuir-Blodgett (LB) films of P(VDF-TrFE) 70:30 copolymers.[11] LB films up to one monolayer thick were shown to exhibit very good P-E loops with a very high coercive field. It was claimed[11] that the P-E loops in LB films correspond to intrinsic (thermodynamic) switching. This conclusion was based on the fact that the coercive field obtained from hysteresis loops at small thicknesses matched that obtained from a homogeneous LGD model that was parametrized from independent measurements on LB films (the homogeneous LGD coercive field is the theoretical limit or the maximum possible value of the coercive field that can be obtained by homogeneously switching all dipoles). However, this claim has been disputed in the literature, and the actual mechanism of switching in such ferroelectric polymer thin films is still not well understood.[12–15] Even in a defect-free system, thermal fluctuations will always be present, which can nucleate reverse domains and influence the switching process. In this paper, we use a multiscale approach to study polarization switching as a function of film thickness and switching frequency in order to test if true intrinsic switching is indeed possible in ultrathin films.

 

Since we focus on intrinsic switching, we neglect the effect of static defects on the polarization switching. Similarly, we also assume that the bound charges at the ferroelectric-electrode interface are perfectly compensated such that there are no depolarization effects. These extrinsic effects can significantly influence the polarization switching behavior.[16,17] The exclusion of these extrinsic effects allows us to focus purely on the intrinsic polarization switching mechanisms.

The organization of this paper is as follows: In Sec. II, we discuss the homogeneous LGD model for ferroelectric phase transition in P(VDF-TrFE) copolymers. MD simulations for P(VDF-TrFE, 70:30) using a modified MSXX force field are performed to obtain the phenomenological coefficients for the LGD model. The intrinsic P-E loop for 70:30 P(VDF-TrFE) is calculated from the homogeneous LGD theory and is compared with that predicted by Ducharme *et al.*[11] Sec. III discusses the TDGL model, describing the kinetics, as well as gradient contributions to the free energy. MD simulations are used to obtain the gradient coefficients, as well as to parametrize the thermal noise, and to set a time scale to the TDGL simulation. In Sec. IV, the TDGL model is used to simulate the polarization switching process by applying a time-dependent electric field. Simulations at different thicknesses and frequencies are performed to understand the polarization switching mechanism.

## II. INTRINSIC COERCIVE FIELD

The intrinsic coercive field of ferroelectric polymers can be calculated from the phenomenological Landau-Ginzburg-Devonshire free energy that can be expressed as

$$f(P_z) = \frac{\alpha_0(T-T_0)}{2}P_z^2 - \frac{\beta}{4}P_z^4 + \frac{\gamma}{6}P_z^6. \tag{1}$$

Here, $P_z$ is the order parameter, which represents the polarization normal to the polymer chains, and $\alpha_0$, $T_0$, $\beta$, and $\gamma$ are the phenomenological parameters. This free energy describes a first-order paraelectric to ferroelectric transition. Ducharme *et al.*[11] obtained the phenomenological parameters from experimental data on LB films and calculated the intrinsic switching loop using Eq. (1). In this work, we obtain the phenomenological parameters via molecular-dynamics simulations (rather than experiment) of the ferroelectric-paraelectric transition for ideal all trans chains of P(VDF-TrFE) (70:30). Here, our goal is to compare the switching loops for this ideal system to the ones measured by Ducharme *et al.*

The methodology used to obtain the coefficients is as follows: Equation (1) has four unknowns. However, we know that $\partial f(P_z)/\partial P_z = 0$ for equilibrium at all temperatures and at the transition temperature $f[P_z(T=T_c)] = f(P_z=0) = 0$, since at $T_c$, the free energy of the ferroelectric phase equals that of the paraelectric phase. Furthermore, if we know the zero-temperature free energy $f_0 = f(T=0)$, the coefficients in Eq. (1) can be obtained as

$$\alpha_0 = [\beta(P_c^2 - P_0^2) - \gamma(P_c^4 - P_0^4)]/T_c,$$

$$T_0 = -T_c(\beta P_0^2 - \gamma P_0^4)/[\beta(P_c^2 - P_0^2) - \gamma(P_c^4 - P_0^4)],$$

$$\beta = 4f_0 P_c^2/(P_c^2 P_0^4 - P_0^6), \tag{2}$$

and

$$\gamma = 3f_0/(P_c^2 P_0^4 - P_0^6). \tag{3}$$

Here $P_0 = P_z(T=0)$ and $P_c = P_z(T=T_c)$.

We perform MD simulations on ideal chains of P(VDF-TrFE) (70:30) to obtain the material constants in Eqs. (2) and (3). The MD simulations are performed using Cerius2 (Ref. 18) together with the force field developed by Abe *et al.*[8] based on the MSXX force field. To obtain the quantities $P_0$, $P_c$, and $T_c$, we performed quasistatic heating starting from an optimized zero-temperature all trans configuration built with four chains—each 10 monomer units long—in the $x$ and $y$ directions (16 chains total) [see Fig. 1; this is akin to the simulations performed by Abe *et al.*[8]]. The temperature was raised in 50 K steps and equilibrated at each step for an additional 45 ps before collecting data for another 55 ps. of the simulations use a 1 fs time step. The MD polarization vs temperature curve is shown in Fig. 2. $P_0$, $P_c$, and $T_c$ can be extracted directly from this plot. The quantity $f_0 = f_\beta - f_\alpha$, where $f_\beta$ and $f_\alpha$ are the energy densities of $\beta$ (ferroelectric) and $\alpha$ (paraelectric phase) at 0 K (the crystal structures of the $\beta$ and $\alpha$ phase at 0 K are shown in Fig. 1). The resulting parameters $P_0$, $P_c$, $T_c$, and $f_0$ are listed in Table I. Table II shows the free-energy parameters obtained using Eqs. (2) and (3) and the parameters in Table I.

Figure 2 shows the polarization vs temperature curve determined analytically from the free energy in Eq. (1) using the coefficients derived from the MD simulations. This is obtained using the condition $\partial f(P_z)/\partial P_z = 0$, which gives $P_z^2 = [\beta + \sqrt{\beta^2 - 4\gamma\alpha_0(T-T_0)}]/2\gamma$. The $P_z$ vs $T$ curve in Fig. 2 is obtained using this relation. The red part of the curve represents the temperatures for which the ferroelectric is the stable phase, while the black dashed curve represents temperatures for which the ferroelectric state is metastable. The corresponding MD data (filled circles) are also plotted to compare with the LGD prediction. Note that in this analysis, we have assumed the temperature, at which the MD polarization drops to zero, is $T_c$ for the LGD model. At this temperature, the ferroelectric and paraelectric states have the same free energy. Above $T_c$, the ferroelectric state is assumed to be metastable with respect to the stable paraelectric state. Thus, we have assumed that in the MD simulations, above $T_c = 450$ K, the metastable ferroelectric state rapidly decays to stable paraelectric phase by a nucleation process that occurs within 100 ps. Although we have performed slower heating runs and found no change in the temperature at which the polarization in the MD simulations drops to zero, our determination of the transition temperature could still be an overestimate (i.e., it should be viewed as an upper bound). The free energy in Eq. (1) can be used to calculate the intrinsic switching loop, i.e., the homogeneous reversal of the polarization. Figure 3 shows the calculated thermodynamic switching loop and that obtained using the LGD parameters in (Ref. 11). The two loops are clearly different. In particular, our coercive field is about three times larger than the intrinsic coercive field of Ducharme *et al.*[11] This may be associated with the approximate/empirical nature of the force field em-

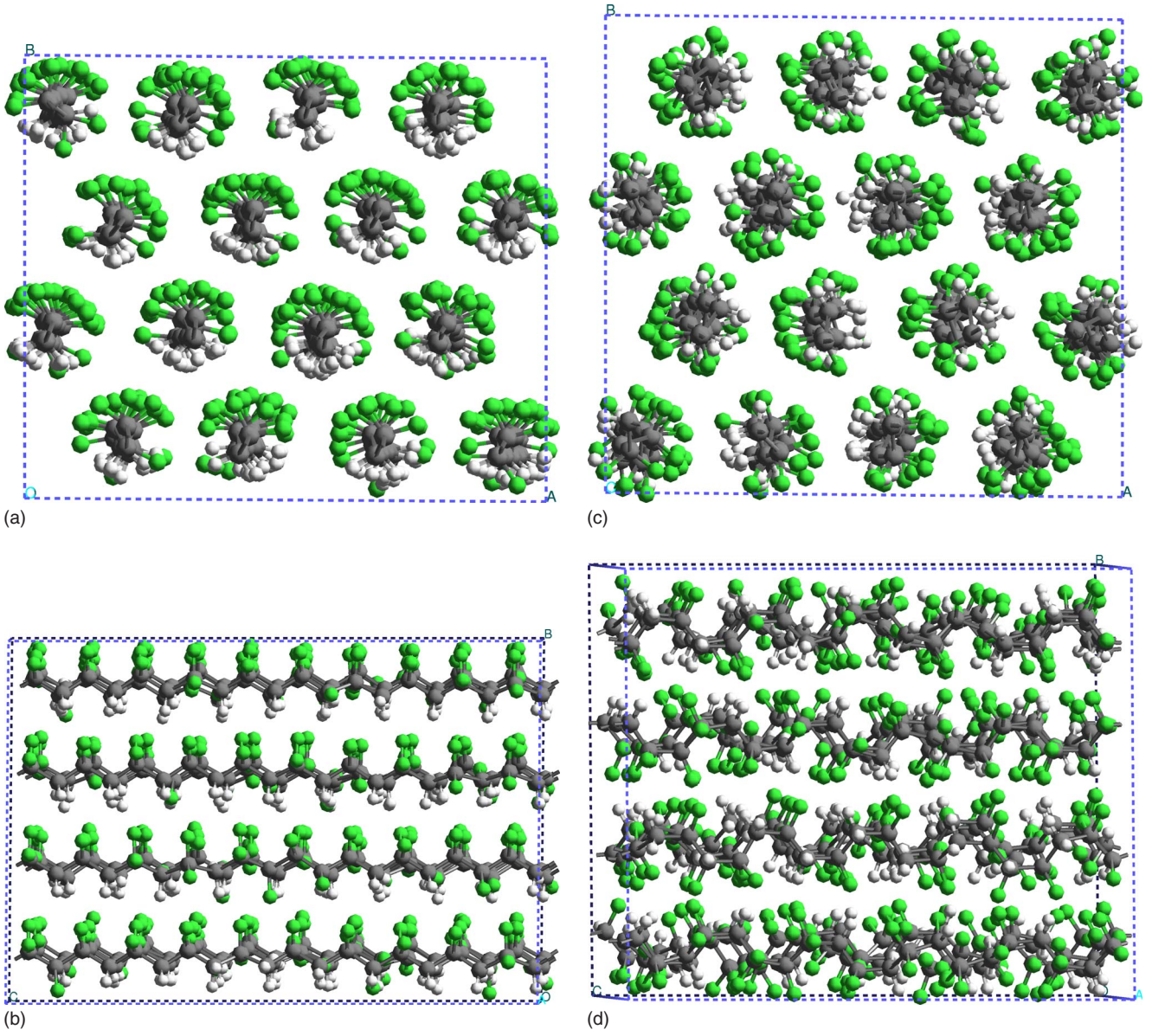


FIG. 1. (Color online) Simulation cell at 0 K for the ferroelectric $\beta$ phase [(a) front and (b) side views] and the paraelectric $\alpha$ phase [(c) front and (d) side views].

ployed and the fact that our material is purely crystalline. The uncertainty in the value of $T_c$ could also contribute to this discrepancy. Since our fitting procedure uses the $T_c$ as an input, our results have a higher intrinsic coercive field value.

## III. DOMAIN WALLS, THERMAL FLUCTUATIONS, AND KINETICS

In general, polarization switching in ferroelectrics involves nucleation and motion of domain walls.[19] In addition, even in the ultrathin (monolayers) films studied by Ducharme *et al.*,[11] thermal fluctuations can make an important contribution to polarization switching. Therefore, the homogeneous analysis of the previous section may be inadequate to accurately address polarization switching. Thus, a kinetic framework—which accounts for domain-wall energy and thermal fluctuations—is essential. We consider a three-dimensional (3D) film with polymer chains oriented along the $y$ axis and the spontaneous polarization oriented along the $z$ axis. The kinetics is simulated within the TDGL framework;

$$\frac{\partial P_i}{\partial i} = -\Gamma_i \frac{\delta F}{\delta P_i} + \eta_i(\vec{r},t) \quad i = x,y,z, \tag{4}$$

where $\Gamma_i$ are kinetic coefficients and $\eta_i(\vec{r},t)$ is a random thermal noise at temperature $T$ given by the fluctuation-dissipation theorem as

$$\langle \eta_i(\vec{r},t) \rangle = 0,$$

$$\langle \eta_i(\vec{r},t)\, \eta_i(\vec{r}',t') \rangle = 2k_b T \Gamma_i \delta(\vec{r}-\vec{r}')\, \delta(t-t'). \tag{5}$$

The free energy $F$ is given by

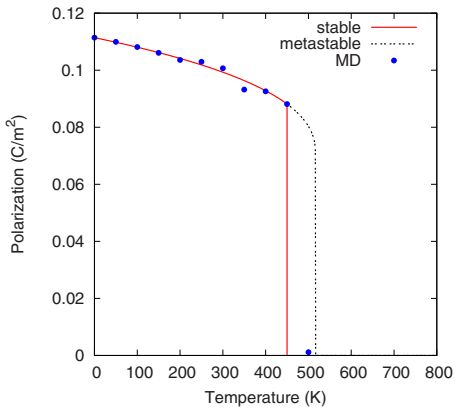


FIG. 2. (Color online) Polarization vs temperature calculated from the LGD model. The red curves correspond to stable ferroelectric phase and the black dashed curve corresponds to the ferroelectric state being metastable. The MD results are also shown as filled circles.

$$F = \int d\vec{r}\left[f(P_z) + \frac{K_1}{2}\left(\frac{\partial P_z}{\partial x}\right)^2 + \frac{K_2}{2}\left(\frac{\partial P_z}{\partial y}\right)^2 + \frac{K_3}{2}\left(\frac{\partial P_z}{\partial z}\right)^2 + \frac{1}{2\chi_{xx}}P_x^2 + \frac{1}{2\chi_{yy}}P_y^2\right] + F_{\text{dep}}, \tag{6}$$

where $f(P_z)$ is the homogeneous free-energy density given in Eq. (1) and the depolarization energy is expressed as

$$F_{\text{dep}} = -\int d\vec{r}\left[\frac{\varepsilon_0}{2}(\vec{E}_{\text{dep}} \cdot \vec{E}_{\text{dep}}) + \vec{E}_{\text{dep}} \cdot \vec{P}\right], \tag{7}$$

with $E_{\text{dep}} = -\vec{\nabla}\phi$, $\phi$ is the electrostatic potential, and $\varepsilon_0$ is the permittivity of free space. Furthermore, the constraint $\vec{\nabla} \cdot \vec{D} = 0$ in the absence of free charge, where $\vec{D} = \varepsilon_0\vec{E} + \vec{P}$ gives

$$-\varepsilon_0\nabla^2\phi + \vec{\nabla} \cdot \vec{P} = 0, \tag{8}$$

In Eq. (6), $\chi_{yy}$ is the susceptibility along the chain and $\chi_{xx}$ that transverse to the chain. In this paper, we make the assumption $\chi_{xx} = \chi_{yy} = \chi_{zz}$, where $\chi_{zz}$ can be evaluated from Eq. (1) as $\chi_{zz} = (\partial^2 f/\partial P_z^2)^{-1}$ evaluated at $P_z = P_r$ (where $P_r$ is the remnant polarization at that temperature). Moreover, it is known for pure PVDF that the susceptibilities along normal and transverse to the chains are approximately equal.[7] The gradient coefficients $K_1$ and $K_2$ are related to the energy cost in creating polarization gradients in the transverse direction and along the chain, respectively, whereas $K_3$ measures the energy cost in creating gradients along the polar direction.

TABLE I. Parameters obtained from MD simulations.

| $P_0$ (C/m$^2$) | $T_C$ (K) | $P_c$ (C/m$^2$) | $f_0$ (J/m$^3$) |
|---|---|---|---|
| 0.111 | 450 | 0.088 | $-2.12\times10^8$ |

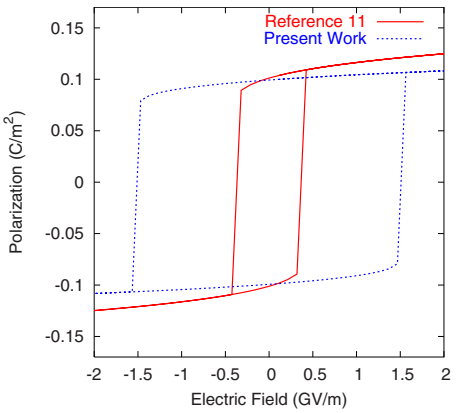


FIG. 3. (Color online) Comparison of the hysteresis loops obtained using the LGD model with the parameters obtained in the present work to that with Ducharme *et al.*

### A. Gradient coefficients

The homogeneous free energy in Eq. (1) was parametrized in Sec. II using molecular-dynamics simulations. To describe inhomogeneities, such as domain walls, we also need to obtain the gradient coefficients $K_1$ and $K_2$ for the P(VDF-TrFE) copolymer. To this end, we make use of the well-known one-dimensional (kink) solution for an isolated 180° domain walls;[20]

$$P_z(x_i) = \frac{P_0 \sinh(x_i/\xi_i)}{\sqrt{A + \sinh^2(x_i/\xi_i)}}, \tag{9}$$

where $i=1$ corresponds to the direction transverse to the chains and $i=2$ refers to the direction along the chain. The polarization $P_0$ is given as $P_0^2 = [\beta + \sqrt{\beta^2 - 4\gamma\alpha_0(T-T_0)}]/2\gamma$ and $A = (6\gamma P_0^2 + 3\beta)/(4\gamma P_0^2 + 3\beta)$. The domain-wall width $\xi_i$ is

$$\xi_i = \frac{\sqrt{K_i}}{\sqrt{\gamma P_0^4 + 0.5\beta P_0^2}}. \tag{10}$$

Thus, we can extract the gradient coefficients $K_1$ and $K_2$ from the domain widths $\xi_1$ and $\xi_2$ (estimated from MD), and $\alpha_0$, $T_0$, $\beta$, and $\gamma$ (already obtained in Sec. II). To do this, we created a simulation cell with two different domains with polarizations differing by 180°. There are two different types of domain walls: one across the chains and one along the chain. We ran our molecular-dynamics simulation for 100 ps for each case. Figure 4(a) shows the 180° domain wall for the case when the domain wall is parallel to the chains and Fig. 4(b) shows the case when the domain wall runs through the chains. Using these results, we estimate $\xi_1 = \xi_2 = 0.4$ nm; this is approximately the separation between chains. Using Eq. (10), we obtain $K_1 = K_2 = 2.108\times10^{-8}$ J m$^3$/C$^2$.

TABLE II. LGD parameters obtained from MD data.

| $\alpha_0$ (J m/C$^2$ K) | $T_0$ (K) | $\beta$ (J m$^5$/C$^4$) | $\gamma$ (J m$^9$/C$^6$) |
|---|---|---|---|
| $9.02\times10^7$ | 252 | $9.20\times10^{12}$ | $8.88\times10^{14}$ |

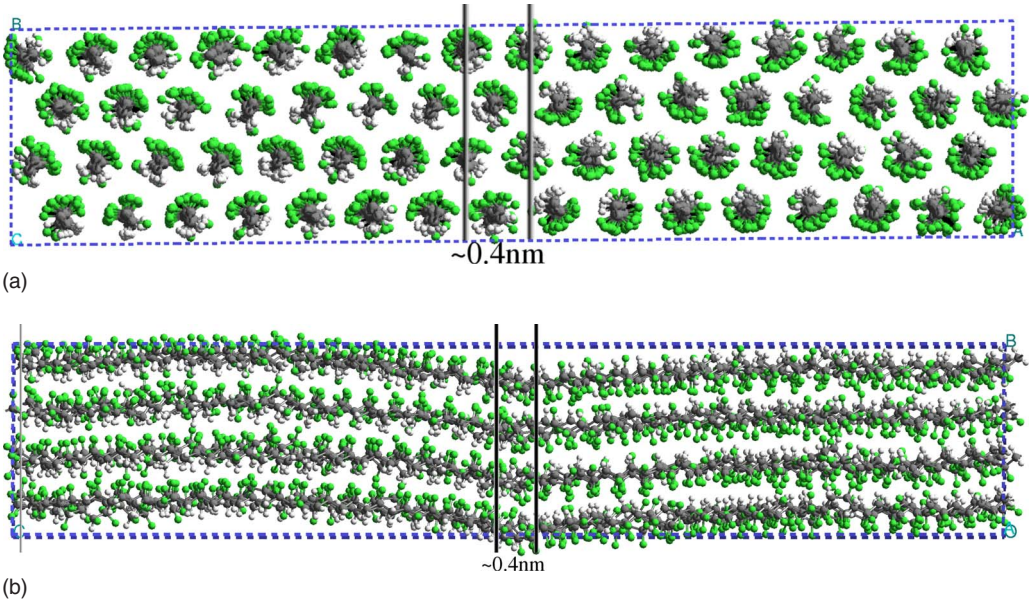


FIG. 4. (Color online) (a) 180° domain wall parallel to the chains and (b) perpendicular to the chains.

To obtain the coefficient $K_3$ from MD would require setting up a domain wall in which the polarizations meet head to head or tail to tail. Such domain walls are highly unstable due to electrostatic energy. This suggests that physics of polarization gradients normal to the chain is governed more by electrostatic energy, in Eq. (7), rather than domain-wall energy. While no such domain walls will exist, we arbitrarily set $K_3=K_1=K_2$ for computational convenience. This approximation of isotropic gradient coefficients does not significantly influence the results in the present paper.

### B. Kinetic parameters: Thermal noise and time scales

We now use the MD simulations to fix the noise amplitude as well as set a time scale for the P(VDF-TrFE) system. To study the kinetics and fluctuations, a P(VDF-TrFE) (70:30) system was suddenly heated to 300 K using MD starting from the optimized configuration at 0 K. Figure 5(a) shows the evolution of $P_z$ with time obtained from the MD simulation.

To obtain the noise amplitude and the time scale for the TDGL model, we simulate a similar situation using Eq. (4). First, the TDGL equations are rescaled by introducing dimensionless parameters as $\vec{P}=P_0(u,v,w)$, $P_0^2=\beta/\gamma$ and $\vec{r}=\delta(x',y',z')$, $\phi=\delta P_0/\varepsilon_0\phi$, $t^*=\Gamma_z\beta P_0^2 t$. With these variable changes, the TDGL equation in Eq. (4) can be expressed as

$$\frac{\partial w}{\partial t^*}=-\left[\alpha' w-w^3+w^5-K_1'\frac{\partial^2 w}{\partial x'^2}-K_2'\frac{\partial^2 w}{\partial y'^2}-K_3'\frac{\partial^2 w}{\partial z'^2}+E'\frac{\partial \phi'}{\partial z'}\right]+\tilde{\varepsilon}_z\tilde{\eta}_z,$$

$$\frac{\partial u}{\partial t^*}=-m\left[\alpha_{xx}' u+E'\frac{\partial \phi'}{\partial x'}\right]+\tilde{\varepsilon}_x\tilde{\eta}_x,$$

$$\frac{\partial v}{\partial t^*}=-n\left[\alpha_{yy}' v+E'\frac{\partial \phi'}{\partial y'}\right]+\tilde{\varepsilon}_y\tilde{\eta}_y. \tag{11}$$

Here $\alpha'=\alpha_0(T-T_0)/\beta P_0^2$, $\alpha_{xx}'=1/(\beta P_0^2\chi_{xx})$, $\alpha_{yy}'=1/(\beta P_0^2\chi_{yy})$, $K_1'=K_1/(\delta^2\beta P_0^2)$, $K_2'=K_2/(\delta^2\beta P_0^2)$, $E'=1/(\varepsilon_0\beta P_0^2)$, and $\tilde{\varepsilon}_z=\sqrt{2k_bT/\beta P_0^4\delta^3}$. The quantities $\tilde{\eta}_i$ are the Gaussian random numbers with unit variance. The kinetic coefficients for $x$ and $y$ components of the polarization are $\Gamma_x=m\Gamma_z$ and $\Gamma_y=n\Gamma_z$, respectively, and the rescaled noise amplitudes along the $x$ and $y$ directions are given by $\tilde{\varepsilon}_x=\sqrt{m}\tilde{\varepsilon}_z$ and $\tilde{\varepsilon}_y=\sqrt{n}\tilde{\varepsilon}_z$.

With the rescaling procedure, the constraint in Eq. (8) can be simplified to

$$-\nabla'^2\phi'+\frac{\partial u}{\partial x'}+\frac{\partial v}{\partial y'}+\frac{\partial w}{\partial z'}=0. \tag{12}$$

Equations (11) subject to the constraint Eq. (12) are solved on a grid to simulate the evolution of the polarization. Periodic boundary conditions are assumed for the polarizations $u,v,w$, as well as for the electrostatic potential $\phi'$. To mimic the MD simulation depicted in Fig. 5(a), the initial polarization is uniformly set to $\vec{P}(T=0K)=(0,0,0.114)\mathrm{C/m}^2$. The simulation cell for the TDGL equations is $138.24\times138.24\times138.24$ nm$^3$ (corresponding to a smallest length scale of 2.16 nm, which is chosen so that the volume of the smallest unit cell of the TDGL simulation is the same as the volume of the MD simulation cell). After making a choice for the noise variables $\tilde{\varepsilon}_x,\tilde{\varepsilon}_y,\tilde{\varepsilon}_z$, the temperature is raised to 300 K and the evolution of the polarization with the rescaled time $t^*$ is monitored. It is observed that after a brief transient, the polarization at all points on the grid saturates and fluctuate around a mean value corresponding to the total polarization at that temperature. The simulations were repeated for several of noise amplitudes (i.e., $\tilde{\varepsilon}_x,\tilde{\varepsilon}_y,\tilde{\varepsilon}_z$) until the mean value and the extent of the polarization fluctuations approximately matches that in the MD

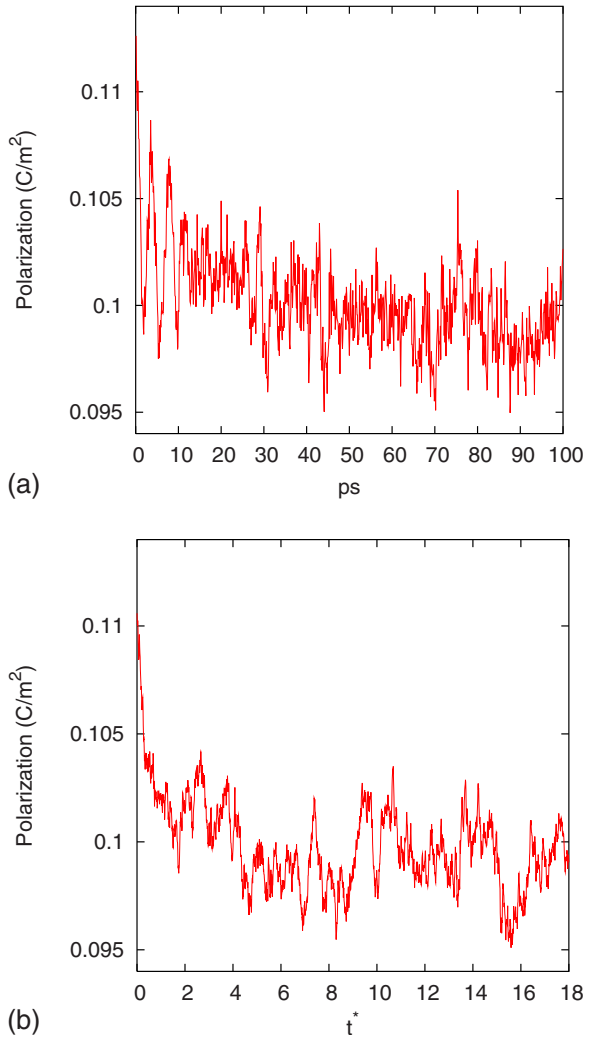


FIG. 5. (Color online) (a) $P_z$ vs time obtained from MD simulations at 300 K starting from the 0 K structure. (b) Evolution of $P_z$ with rescaled time $t*$ at a representative point on the simulation grid of the TDGL simulations.

simulation results shown in Fig. 5(a). The matched result $(\tilde{\varepsilon}_x=0.0711, \tilde{\varepsilon}_y=1.0669, \tilde{\varepsilon}_z=0.3556)$ at a representative grid point is shown in Fig. 5(b) (keep in mind that all grid points on the TDGL simulation grid exhibit similar behavior). Notice that the polarization in the TDGL simulation equilibrates at $t^* \approx 5$, whereas the equilibration time in MD is 45 ps. From this, we set the smallest time scale for the TDGL simulations to be $\approx 9$ ps. This implies that the TDGL equation can be used to access much longer time scales than normally accessible to traditional MD simulations. In the next section, we use the TDGL model to simulate polarization switching, where the fastest switching simulation is run for 100 ns/cycle and the slowest simulation corresponds to 1 $\mu$s/cycle.

## IV. SIMULATION OF POLARIZATION SWITCHING

Since all thermodynamic and kinetic parameters of the TDGL model, as well as the length and time scales, have been set from MD simulations for P(VDF-TrFE) copolymers, we can now simulate the polarization switching process. The simulation procedure is as follows: First, a single domain remnant state is created by solving Eq. (11) subject to the constraint Eq. (12) starting from a trial single domain state on a $h \times (138.24 \times 138.24\ \text{nm}^2)$ grid, where $h$ is the film thickness (as in the simulations performed in Sec. II, the smallest length in this simulation cell is equal to 2.16 nm—which is chosen such that the volume of the smallest unit cell of the TDGL simulation is equal to the volume of the MD simulation cell). Periodic boundary conditions are used for the polarizations along $x$ and $y$ directions. Normal to the film, we use the boundary conditions $\partial P_i/\partial z=0$, where $i=x,y,z$. Note that this corresponds to the condition where surface charge is perfectly compensated and there are no depolarizing fields present. Short circuit boundary conditions $\phi(x,y,z=0,t)=\phi(x,y,z=h,t)=0$ are used. After obtaining a stable single domain state, a time-dependent voltage $\phi(x,y,z=0,t)=0$ and $\phi(x,y,z=h,t)=V_0(h/h_c)\sin(2\pi ft)$ with switching frequency $f$ are then applied to the stable remnant state. Here $h_c=138.24$ nm is a reference thickness. Note that with this choice of the applied potential, the electric field is independent of the thickness. The switching loops are obtained by calculating $\langle P_z \rangle$ vs $\langle E_z \rangle$, where $E_z=-\partial\phi/\partial z$ and the averages are performed over the entire film. Figure 6 shows the simulated hysteresis loop for the $h=10.8$ nm film at a switching frequency $f=11.1$ MHz and $V_0=249$ V. The microstructure snapshots corresponding to points (a)–(f) on the hysteresis loop are also shown. It is clear that polarization switching at the coercive field occurs by a nucleation and growth of reverse domains rather than homogeneous switching of all of the dipoles. Note that no static defects have been introduced in the simulations. Since it is assumed that there is perfect screening of the bound charges at the surface, no depolarization fields exist in the film. This means that the domain formation is purely due to homogeneous nucleation caused by the thermal noise. This figure shows that even at very small thickness, domain nucleation cannot be completely inhibited. We also note that the actual switching time at the coercive field [time elapsed between the points (b)–(f) in Fig. 6] is ~450 ps, which is much smaller than the typical experimental switching times for ferroelectric polymers.[14] This may be attributed to the fact that switching occurs at very high field (almost the intrinsic coercive field) in our simulations, whereas in most experiments the switching may be influenced by defect induced heterogeneous nucleation and occurs at much lower coercive fields.

To further investigate the nature of the switching process, we performed the simulations at three different film thicknesses. It is clear from Fig. 7 that for very thin films, the coercive field does not increase with decreasing film thickness. Note that this is consistent with Ref. 11, where it was found that the coercive field does not depend on the film thickness below a thickness of 15 nm. This was interpreted by Ducharme *et al.* as a realization of intrinsic switching.[11] Our calculations have shown that saturation of the coercive field at small thicknesses does not imply perfectly homogeneous intrinsic switching, as in each case shown in Fig. 7, switching occurs through thermally induced domain nucleation. However, the reduction in the coercive field compared to the intrinsic value is not substantial. We conclude that

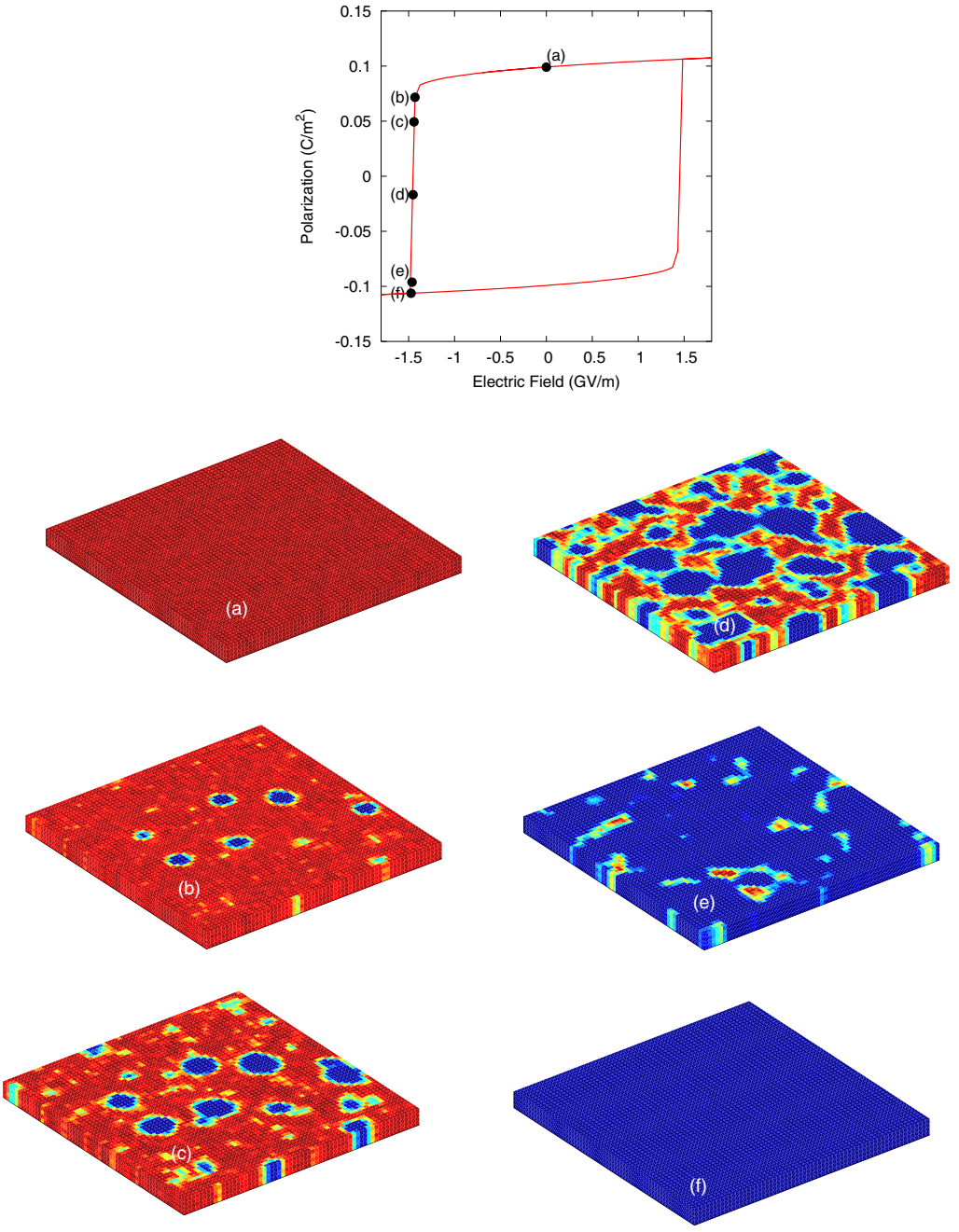


FIG. 6. (Color online) Hysteresis loop for an $h=10.8$ nm film at a switching frequency $f=11.1$ MHz. The domain evolution corresponding to points (a)–(f) are also shown.

although perfectly homogeneous switching may not be possible, coercive field values close to the intrinsic value may be obtained provided that there are no defects and depolarization fields. Defects and depolarization fields could reduce the coercive field even further. The thickness independence of the coercive field is due to the fact that during the switching at the coercive field, reversed polarization domains rapidly propagate (driven by the electrostatic fields due to the bound charges) to the top and bottom surfaces to form columns (as seen in Fig. 6). Thus we do not expect any thickness dependence of the coercive field in a purely defect-free system. We believe that the films smaller than 15 nm, in Ref. 11, exhibit this behavior. For larger thicknesses, nucleation may occur heterogeneously at defects such that the coercive field increases with decreasing thickness due to a decrease in the available nucleation volume.[11]

Since we have shown that thermal fluctuations can lead to reverse domain nucleation, the switching process is expected to depend upon the switching frequency. We performed switching simulations at three different frequencies. The switching loops for these frequencies are shown in Fig. 8. Notice that the coercive field decreases as the switching frequency is decreased. This is due to the fact that more time is available for domain nucleation with slower switching. Although slower switching results in a lowered coercive field, the frequency dependence is weak. We do not expect that

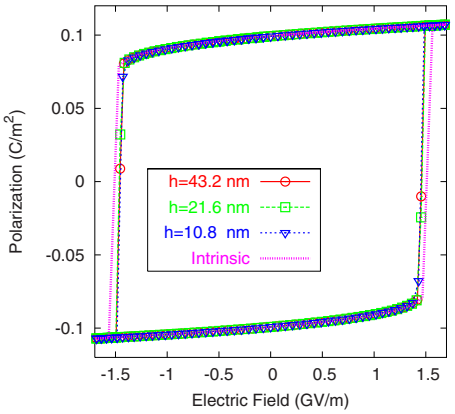


FIG. 7. (Color online) Hysteresis loops for three different thicknesses at frequency $f=11.1$ MHz. The corresponding intrinsic loop is also shown.

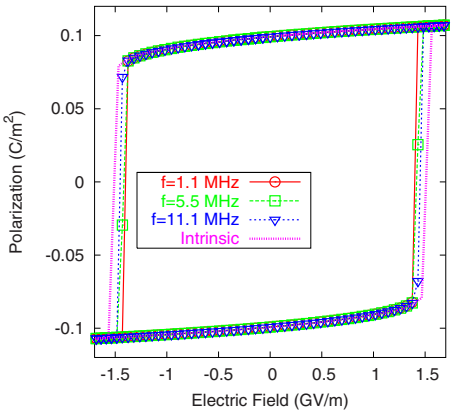


FIG. 8. (Color online) Hysteresis loops for three different frequencies for $h=10.8$ nm. The corresponding intrinsic loop is also shown.

with further reduction in frequency, the coercive field will eventually approach the coercive field as observed by Ducharme *et al.* Additional nucleation mechanisms such as defects would be required to achieve the low coercive field values observed in Ref. 11.

## V. SUMMARY

We have proposed a multiscale framework that parametrizes a continuum model for ferroelectric polymers from information obtained at atomistic scales. The phenomenological parameters, kinetic coefficients, and thermal noise amplitude for a mesoscale time-dependent Ginzburg-Landau model are obtained from MD simulations that employ a force field fit to macroscopic behavior. The framework developed described herein is generic and can be applied to other ferroelectric materials, as well as other phase transitions that can be described by Landau theory.

The multiscale framework is applied to study polarization switching in P(VDF-TrFE) ferroelectric polymer thin films, focusing on the issue of achievability of intrinsic (homogeneous) polarization switching in very thin films. The intrinsic switching loop is calculated using the homogeneous Landau-Ginzburg-Devonshire theory, the phenomenological parameters for which are obtained from MD simulations. The intrinsic loop is compared with that determined by Ducharme *et al.* using parameters obtained from data on Langmuir-Blodgett films of 70:30 P(VDF-TrFE) copolymers. It is found that the intrinsic coercive field predicted by the present multiscale model is about three times higher than the one obtained by Ducharme *et al.* To investigate the role of thermal fluctuations and kinetics, simulations of the switching process were performed at different film thicknesses and switching frequency. It is found that the coercive field is independent of film thickness at small thicknesses. This is consistent with the results of Ducharme *et al.* who found that the coercive field does not increase below a thickness of 15 nm. However, the switching process occurs by domain nucleation even for very thin films although this nucleation does not significantly decrease the coercive field compared to the intrinsic value. Thus we conclude that coercive fields very close to the intrinsic coercive field may be observed in ferroelectric polymer thin films provided that the defect density within the film or depolarization effects are not too large.

[1] T. Furukawa, Phase Transitions **18**, 143 (1989).
[2] *Ferroelectric Polymers : Chemistry, Physics, and Applications*, edited by H. S. Nalwa (Dekker, New York, 1995).
[3] H. Kawai, Jpn. J. Appl. Phys. **8**, 975 (1969).
[4] T. J. Reece, S. Ducharme, A. V. Sorokin, and M. Poulsen, Appl. Phys. Lett. **82**, 142 (2003).
[5] W. Zhang and K. Bhattacharya, Acta Mater. **53**, 185 (2005).
[6] J. Y. Jo, D. J. Kim, Y. S. Kim, S. B. Choe, T. K. Song, J. G. Yoon, and T. W. Noh, Phys. Rev. Lett. **97**, 247602 (2006).
[7] N. Karasawa and W. A. Goddard III, Macromolecules **25**, 7268 (1992).
[8] Y. Abe, K. Tashiro, and M. Kobayashi, Comput. Theor. Polym. Sci. **10**, 323 (2000); Y. Abe and K. Tashiro, Polymer **42**, 3409 (2001); Y. Abe and K. Tashiro, J. Polym. Sci., Part B: Polym. Phys. **39**, 689 (2001); T. Abe and K. Tashiro, Polymer **42**, 9671 (2001).
[9] N. Karasawa and W. A. Goddard III, Macromolecules **28**, 6765 (1995).
[10] H. Su, A. Strachan, and W. A. Goddard III, Phys. Rev. B **70**, 064101 (2004).
[11] S. Ducharme, V. M. Fridkin, A. V. Bune, S. P. Palto, L. M. Blinov, N. N. Petukhova, and S. G. Yudin, Phys. Rev. Lett. **84**, 175 (2000).
[12] A. M. Bratkovsky and A. P. Levanyuk, Phys. Rev. Lett. **87**, 019701 (2001).
[13] R. L. Moreira, Phys. Rev. Lett. **88**, 179701 (2002).
[14] H. Kliem and R. Tadros-Morgane, J. Phys. D **38**, 1860 (2005).
[15] R. C. G. Naber, P. W. M. Blom, and D. M. de Leeuw, J. Phys. D

**39**, 1984 (2006).
[16] D. J. Kim, J. Y. Jo, T. H. Kim, S. M. Yang, B. Chen, Y. S. Kim, and T. W. Noh, Appl. Phys. Lett. **91**, 132903 (2007).
[17] R. Ahluwalia and D. J. Srolovitz, Phys. Rev. B **76**, 174121 (2007).
[18] CERIUS2, Version 4.7., Accelrys, Inc.
[19] W. J. Merz, Phys. Rev. **95**, 690 (1954).
[20] W. W. Cao and L. E. Cross, Phys. Rev. B **44**, 5 (1991).